PERGAMON

Deep-Sea Research II 48 (2001) 1303–1323

DEEP-SEA RESEARCH
PART II

www.elsevier.com/locate/dsr2

Heterotrophic bacterioplankton in the Arabian Sea: Basinwide response to year-round high primary productivity

H.W. Ducklow[a,*], D.C. Smith[b], L. Campbell[c], M.R. Landry[d], H.L. Quinby[a], G.F. Steward[e], F. Azam[f]

[a]*The College of William and Mary School of Marine Science, PO. Box 1346, Gloucester Point, VA 23062, USA*
[b]*University of Rhode Island Graduate School of Oceanography, Narragansett, RI 02882, USA*
[c]*Department of Oceanography, Texas A&M University, College Station, TX 77843, USA*
[d]*Department of Oceanography, University of Hawaii, Honolulu, HI 96822, USA*
[e]*Monterey Bay Aquarium Research Institute, Moss Landing, CA 95039, USA*
[f]*Scripps Institution of Oceanography, La Jolla, CA 92093, USA*

Received 17 December 1998; received in revised form 22 October 1999; accepted 19 November 1999

Abstract

Heterotrophic bacterial abundance and productivity were measured during five and four cruises, respectively, in the northwest Arabian Sea as part of the US JGOFS Process Study, which provided a new view of seasonal bacterial dynamics in that part of the basin influenced by monsoonal forcing. In this paper, surface layer data are used to address two questions concerning the influence of the monsoon cycle on bacterial dynamics: (1) Is there a bacterial bloom in the SW Monsoon? and (2) Is bacterial production low during the oligotrophic Spring Intermonsoon? An extensive comparison of epifluorescence microscopy and flow cytometry, unprecedented at this scale, detected essentially the same heterotrophic bacterial populations and distributions, with some between-cruise differences. Use of the two methods allowed us to extend our observations in space and time. Bacterial productivity, both in the surface layer and integrated over the euphotic zone, was elevated less than 2-fold during the Southwest Monsoon. Levels of bacterial abundance and production were low during the Northeast Monsoon, then increased in March during the Spring Intermonsoon. There was some stimulation of abundance or production inshore in response to coastal upwelling. In general, the basin was enriched in bacterial biomass $> 5 \times 10^8$ cells l^{-1} throughout the year, relative to other tropical regimes, presumably in response to overall high PP and DOC levels. Seasonally uniform DOC levels may be regulated in part by intense bacterial utilization rates, but also reflect seasonal consistency in PP.

* Corresponding author. Fax: +1-804-684-7293.
E-mail address: duck@vims.edu (H.W. Ducklow).

0967-0645/01/$ - see front matter
PII: S0967-0645(00)00140-5

1. Introduction

The Arabian Sea is unique among the world's major ocean basins. It is a relatively small ocean basin, closed to the north, which restricts circulation and exchange, leading to an extensive volume of hypoxic water beneath the seasonal pycnocline (Olson et al., 1993). Moreover, the basin experiences extreme wind forcing from seasonally reversing monsoonal winds (Smith et al., 1991). The Southwest (SW) Monsoon (June–September) drives coastal upwelling, which relaxes in the following Fall Intermonsoon season (October–November), leading to alternating mesotrophic and oligotrophic phases in the euphotic zone. Based on CZCS data, the Arabian Sea appears to have the highest seasonal variability in surface chlorophyll (Yoder et al., 1993) and primary productivity (PP, Brock et al., 1993, 1994) of any tropical oceanic basin. For example, Brock et al.'s (1993, 1994) model suggested a seasonal range in PP of $< 300- > 2500\,\mathrm{mg\,C\,m^{-2}\,d^{-1}}$ (25–210 mMol $\mathrm{C\,m^{-2}\,d^{-1}}$) north of 10° North. The small size and predictable, enhanced seasonality of the Arabian Sea made it an interesting and useful place in which to examine the responses of plankton communities and the biogeochemical system to changes in physical forcing and carbon inputs (Smith et al., 1991).

In this regard, the Arabian Sea is also a useful region for investigating the responses and regulation of bacterioplankton. We originally hypothesized that bacterial activity would vary in response to extreme primary production variations forced by the monsoonal cycle. Thus, we wanted to know if high primary production rates driven by coastal upwelling during the SW Monsoon caused a notable bacterial response. Further, we did not know previously if bacterial properties declined during the intermonsoonal seasons (oligotrophic phases).

A more thorough examination of the general relationship between bacteria, physics and phytoplankton required a comprehensive and extensive expedition to the northern Arabian Sea. In particular, there was a need to sample during the SW Monsoon. The opportunity to examine these questions is now possible with data from the JGOFS Arabian Sea Process Study (Smith et al., 1991, van Weering et al., 1997; Burkill, 1999). JGOFS' observations commenced with the Dutch expeditions during May 1992–February 1993 in the Somali upwelling region and surrounding coastal ocean, during the SW and Northeast (NE, December–February) Monsoons. The British ARABESQUE Expedition occupied stations in the northern Arabian Sea in August–December, 1994. Both expeditions sampled during the SW Monsoon. Bacterial measurements were made during both expeditions (Goosen et al., 1997; Wiebinga et al., 1997; Pomroy and Joint, 1998). German JGOFS and US JGOFS again occupied the basin in 1995. As a result, we can now attempt a more complete examination of the seasonal course of bacterial and primary production. We made observations of heterotrophic bacterial stocks and production during the NE Monsoon (January and December), the Spring Intermonsoon (March) and the SW Monsoon (July and August). Campbell et al. (1998) have compared stocks and vertical and horizontal variations of picoplankton, including heterotrophic bacteria, on the same cruises. In this paper, we present observations on the geographic distribution of bacterial abundance and production to illustrate the spatial and temporal patterns of bacterial responses to the seasonal changes in physical forcing, nutrients and phytoplankton. Furthermore, we make use of two complementary data sets on bacterial abundance obtained by both flow cytometric and epifluorescence microscopic estimates.

2. Materials and methods

The US JGOFS Arabian Sea Expedition was conducted from January to December 1995 aboard R/V *T. G. Thompson*. The five Process Cruises considered here (TN043, TN045, TN049, TN050, TN054) each occupied the stations shown on the map in Fig. 1. The stations were arranged along northern (N) and southern (S) transect lines extending from near the Omani coast into the oligotrophic tropical Indian Ocean near 10°N, 65°E. Stations S11 and S13 were close (within 10 nm) to Stations 4 and 5 occupied by the R. R. S. *Darwin* in September 1986 (Ducklow, 1993); and Stations S1–13 were located near R. R. S. *Darwin*'s cruise track A1–10 of Sept.–Dec. 1994 (Pomroy and Joint, 1998). The cruise track consisted of short (< 6 h) CTD stations with limited hydrographic sampling and medium (6–12 h), and long (1–2 d) experimental stations at which the full suite of JGOFS measurements were made, including in situ primary production. Core hydrographic data (e.g., T, S, O_2, CO_2, nutrients, Chl *a*) were collected at all stations, whereas bacterial rate measurements and microscopic abundance measurements were made only at medium and long stations. Flow cytometric determinations of bacterial abundance were made at all stations during TN050 and TN054, but not on TN043 and TN045 (cf. Station dots in Figs. 1 and 4). All samples discussed here were collected from a CTD-Rosette fitted with 24, 10-l modified Niskin-type bottles (Morrison et al., 1998). Most data reported in this paper were drawn from surface bottles closed just below the surface (ca. 1 m). Selected data are presented from deeper samples in the water column. Water samples were not prescreened prior to processing described below.

Hydrographic properties were sampled and analyzed as described in Morrison et al. (1998). Chlorophyll *a* was determined using HPLC as described in Goericke and Repeta (1993) and Latasa et al. (1996). Mixed layer depths were estimated using the $\Delta\sigma_t > 0.125$ criterion (Gardner et al., 1999) and obtained from the US JGOFS database.

Bacterial abundance and biovolume were determined microscopically, following JGOFS Protocols (Knap et al., 1996). Samples were preserved with particle-free (0.2 μm filtered) 25% glutaraldehyde (2% final conc.) and stored in a refrigerator until slide preparation. All slides were prepared within 48 h of collection. A volume of each sample sufficient to deposit 15–30 cells within the 24×24 μm field of view of the video camera at 1250X (see below) was filtered onto a prestained, 0.2 μm pore size black polycarbonate filter (Poretics Corp.) in an all-glass filtration assembly. Backing filters (0.45 μm, mixed ester) were used under the Poretics filters to ensure even distribution of cells. Samples were stained with 0.005% acridine orange after Hobbie et al. (1977) and mounted on microscope slides using Resolve ® Immersion Oil and stored at -20°C in slide boxes. Bacterial abundances and biovolumes were estimated for the March and July cruises using a Zeiss Axiophot epifluorescence microscope, equipped with a solid state video camera (Photometrics CH250 CCD) and ImagePro image analysis system in Ducklow's laboratory (Bjornsen, 1986; Ducklow et al., 1995). We used blue excitation (450–490 nm) from a 200 W mercury lamp, with a 510 nm beam splitter and a 520 nm emission filter. Sufficient video images were acquired on each slide to yield about 300–600 measurements of individual cells. Apparent cell volume was derived using an algorithm derived from image analysis estimates of cell axes, area and perimeter, which avoids large error resulting from cubing linear dimensions (Ducklow et al., 1995). One slide was made and analyzed per sample for most experiments. Between-operator estimates of total biovolume (abundance times mean cell volume) vary by 5–10%. For the January and December

cruises, samples were enumerated visually on an Olympus BH2 epifluorescence microscope in Azam's laboratory. Biovolumes were not determined for these cruises.

Water samples for flow-cytometric (FCM) analyses of microbial populations were preserved in 3-ml cryogenic tubes with paraformaldehyde (final concentration 1%) and frozen in liquid nitrogen. FCM samples were thawed and stained with Hoechst 33342 ($0.8\,\mu g\,ml^{-1}$ final concentration) for 30 min before analysis of picoplankton populations (Monger and Landry, 1993). Subsamples of 100 μl were enumerated on a Coulter EPICS 753 flow cytometer equipped with dual argon lasers, MSDS II automatic sampling, and Cicero CYTOMATION software. The lasers were aligned colinearly with the first laser tuned to the UV range to excite Hoechst-stained DNA. The blue fluorescence from the DNA stain distinguished cells from nonliving particulate matter. The second laser was tuned to 488 nm at 1.3 W to excite the pigments of autotrophic cells. This configuration allowed heterotrophic bacterial cells to be readily distinguished from co-occurring phototrophic bacteria (*Prochlorococcus* spp.) in the same size range (measured as forward and right-angle light scattering properties). All FCM samples were spiked with a standard mixture of Polysciences Fluoresbrite YG 0.57- and 0.98-μm visible beads and 0.46-μm UV beads to normalize cellular properties between runs.

Bacterial production rates were estimated from determinations of the rates of incorporation of methyl-^{3}H-thymidine (TdR; specific activity $> 80\,Ci\,mmol^{-1}$) and 2,3-^{3}H-leucine (Leu; specific activity $> 140\,Ci\,mmol^{-1}$; both from New England Nuclear) using the microcentrifugation protocol (Smith and Azam, 1992). All surface samples were incubated within 1°C of the in situ temperature in the dark in refrigerated circulator baths. In this method 1.7-ml samples are incubated in 2-ml polypropylene screw-capped centrifuge tubes held in the bath in floating racks. Surface samples were incubated for 0.5–2 h depending on anticipated incorporation rates. Incorporation was linear over this period (data not shown, but see Ducklow, 1993; Wiebinga et al., 1997) Triplicate subsamples and zero-time blanks were run for all samples. All samples were extracted twice in cold 5% trichloroacetic acid and rinsed with 80% ethanol by sequential decanting, washing and recentrifugation before liquid scintillation counting in Packard Ultima Gold ® cocktail. All LSC counting was completed on board the ship in a Beckman LS 6000 instrument. Analytical precision for triplicate incubations (standard deviation/mean) for TdR and Leu incorporation averaged 0.22 and 0.20, respectively ($n = 843$).

Bacterial abundance was determined by both methods on all cruises except the SW Monsoon cruises. There were no cytometric determinations of heterotrophic bacterial abundance made on the July cruise and no epifluorescence determinations on the August cruise. In addition no bacterial activity measurements were included on the August cruise. Thymidine and leucine incorporation rate determinations were limited to the South Transect on the July cruise, as a result of problems shipping radioisotopes through Oman Customs prior to the cruise.

All data were contoured in Surfer 6.01 (Golden Software, Golden, CO). Data were gridded using a Kriging algorithm, set to search all data points in a 15° latitude by 14° longitude array with 0.2° spacing, a linear variogram and no anisotropy, as in standard topographic applications. For most hydrographic data all stations were sampled (Figs. 1and 2), but for the bacterial data fewer stations were sampled which resulted in sparser coverage (Figs. 4–7). To test the effects of sparser data arrays on gridding results, we compared a temperature data set gridded with all stations to the same one gridded and contoured after removing stations so the map resembled a typical bacterial data set (cf. Figs. 2 and 4). The mean residuals between estimated temperature at the grid point

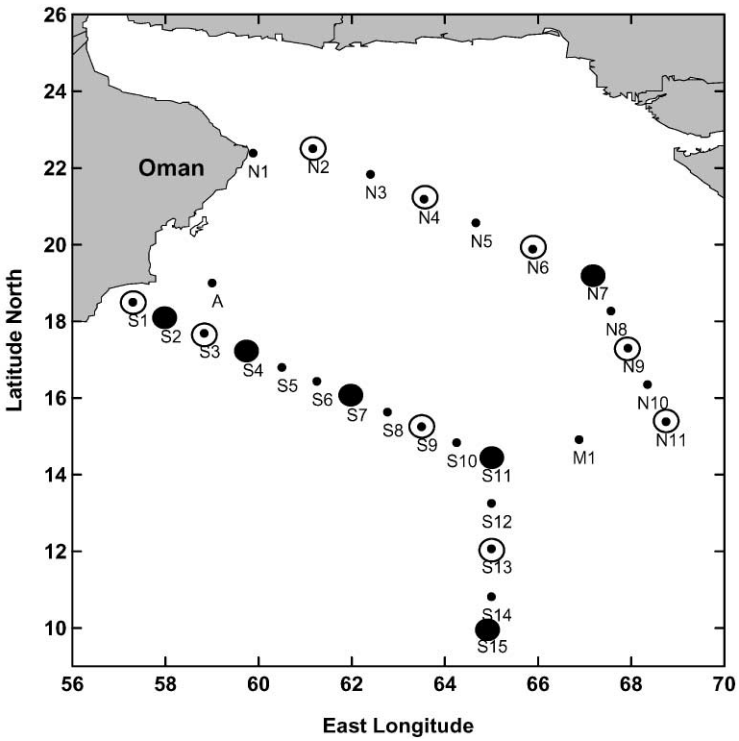

Fig. 1. CTD (small solid circles) and longer rate process stations (large open and closed circles) occupied during the US JGOFS Arabian Sea Expedition, January–December, 1995. Large solid circles show stations where in situ primary production was measured. Bacterial production and microscopy were sampled at all large circles.

nearest each station and the observed temperature were computed for the complete and subsampled maps. The contour map for the incomplete station array and the full array were very similar and the means of the residuals did not differ significantly ($p > 0.05$).

3. Results

3.1. Seasonal evolution of surface hydrographic properties

Hydrography, winds and biological properties of the study area have been presented in other recent papers from the various JGOFS Expeditions (Morrison et al., 1998). Here we provide a brief survey of some principal observations by our colleagues drawn from the US JGOFS database to provide a context in which to view the seasonal and geographic patterns of bacterial properties. The sampling grid consisted of two transect lines extending from near the Oman coast about 1500 km into the center of the basin (Fig. 1). This station arrangement provided a large-scale view of surface properties as they vary onshore-offshore and north to south on a seasonal basis (Fig. 2). Surface temperatures were nearly uniform across the region during the late NE Monsoon in

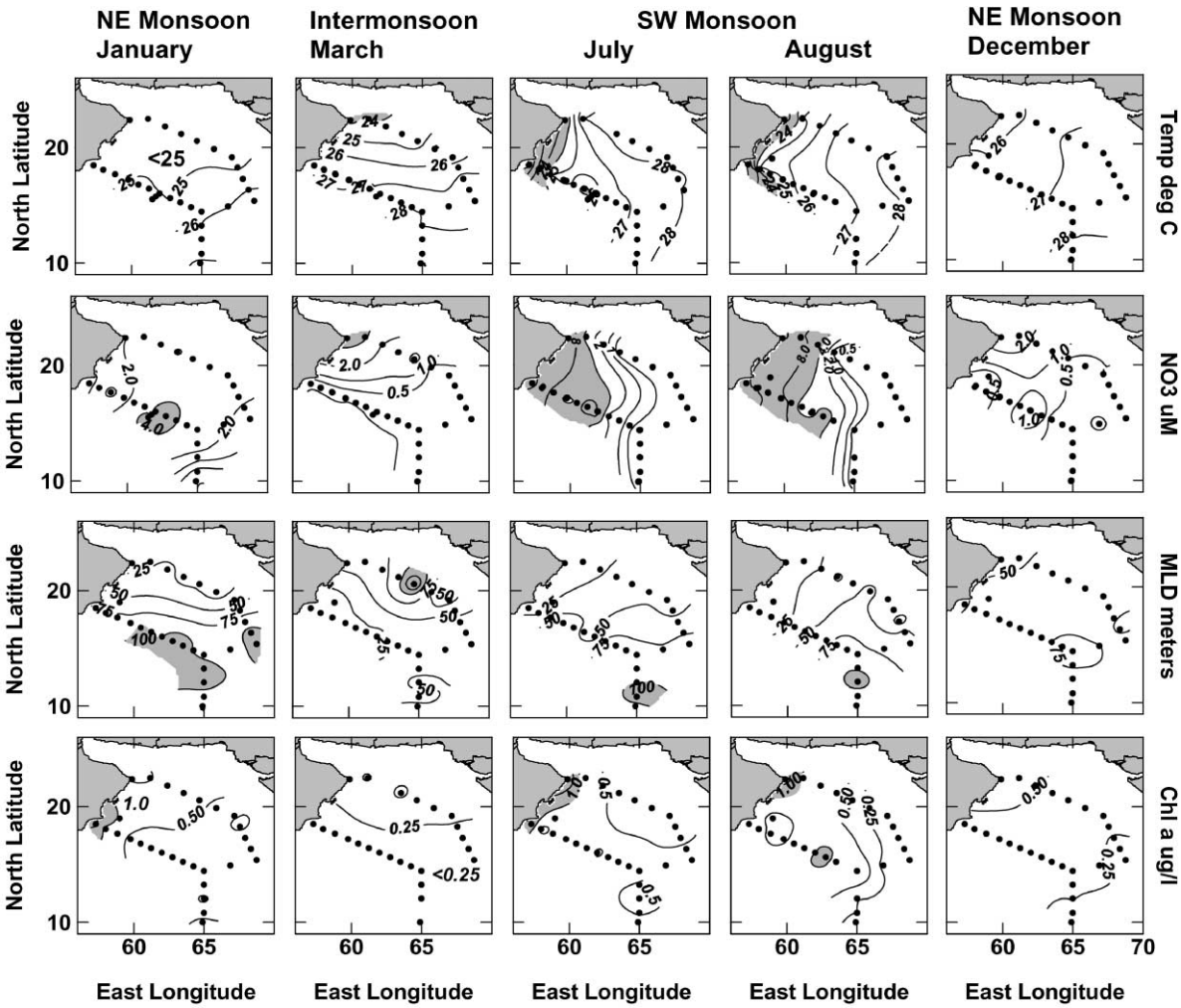

Fig. 2. Physical properties and chlorophyll *a* distributions in the surface of the northern Arabian Sea, January–December, 1995. Top row: temperature, contour interval 1°C, shaded areas less than 24°C; second row, nitrate, contour intervals 0.5–1–2–4–8–16 μmol l^{-1}, shaded areas greater than 4 μmol l^{-1}; third row, mixed layer depth, contour interval 25 meters, shaded areas, greater than 100 meters; bottom row, chlorophyll *a*, contour interval 0.5 μg l^{-1} with 0.25 μg l^{-1} included, shaded areas greater than 1 μg l^{-1}. Data shown here were all obtained from the US JGOFS database at http://usjgofs.whoi.edu/.

January (Fig. 2), and nitrate was 2–4 μg at l^{-1} in the surface layer throughout the study area, except well offshore. Chlorophyll *a* concentrations were around 0.5 μg l^{-1}. During the Spring Intermonsoon (March) there was a more pronounced temperature gradient, and shallower mixed layers $\leqslant 50$ m offshore due to vernal warming, with nitrate < 1 μg at l^{-1} except inshore, and chlorophyll *a* < 0.5 μg l^{-1} (Fig. 2, March column). During the SW Monsoon (Fig. 2, July and August panels), upwelling caused lower temperatures (< 24°C) and high nitrate (> 8 μg at l^{-1}) inshore (*shaded*

areas), with more pronounced mixed layer gradients and higher chlorophyll *a* ($>1\,\mu g\,l^{-1}$) confined to the low temperature, upwelling region. Although nitrate $>4\,\mu g$ at l^{-1} extended into the central basin throughout the SW Monsoon cruises in July–early September, corresponding areas of higher chlorophyll *a* were not observed. During the following early phase of the next NE Monsoon (Fig. 2, December column), surface distributions were again similar to those observed the previous January, with perhaps shallower mixed layers. Mixed-layer depths ranged from <25 to $>75\,m$, with some areas $>100\,m$. Surface chlorophyll *a* was seldom $>2\,\mu g\,l^{-1}$, or $<0.2\,\mu g\,l^{-1}$during the entire study period. This lack of a wide range of chlorophyll *a* levels in the surface was a surprising observation, inconsistent with expectations about pronounced oligotrophic to mesotrophic shifts driven by the monsoonal cycle. Otherwise, hydrographic observations generally adhered to our expectations for the annual cycle in the region.

3.2. Comparison of bacterial abundance estimates

We obtained simultaneous estimates of heterotrophic bacterial abundance using two independent methods on the January, March and December cruises, when samples for both epifluorescence microscopy and flow cytometry were collected at most stations in the upper 200 m (Figs. 3 and 4). The estimates were significantly correlated in all three months, but the relationship varied. The Model II regression slope was 0.99 in January (95% CI: 0.85–1.15, $n = 142$) but the relationship was poor above an abundance of ca. 5×10^8 cells l^{-1}. The relationship between estimates was more consistent across the observed range of abundance in March and December ($r^2 = 0.72$, 0.85, respectively), but slopes differed from 1 (March and December 95% CI: 0.51–0.65, $n = 116$ and 1.27–1.43, $n = 157$, respectively). Thus in March and December, the two methods detected different portions of the heterotrophic bacterial assemblage (Fig. 3), probably owing to changing characteristics of the populations, and differential detection of these changes by each method. The 95% CI for the Model II regression slope for all data combined from all cruises was 0.98–1.12 ($r^2 = 0.689$, $n = 421$), suggesting that over all stations, depths and cruises the two methods were detecting comparable populations of heterotrophic bacteria. The *Y*-intercept was not significantly different from zero ($p < 0.05$). The relatively poor r^2 might be the result of analytical variability of the two techniques, which is about $\pm 15\%$ for each method (Knap et al., 1996; Campbell et al., 1998).

3.3. Spatial distributions of bacterial properties: abundance

Microscopic and flow cytometric determinations of bacterial abundance showed generally similar distribution patterns and a consistent picture of the seasonal evolution of surface bacterial levels (Fig. 4), at least to the level of resolution presented here (5×10^8 cells l^{-1}, or about 25% of peak abundances, see Fig. 3). There were some regional and local scale differences as pointed out below and as shown in Fig. 4. In January, during the late NE Monsoon, abundances were between 5 and 10×10^8 cells l^{-1} by both methods, uniformly distributed across the study area, with no on-to offshore gradient (Fig. 4, top two rows). Surface abundances increased by a factor of 2 during the Spring Intermonsoon in March, with more noticeable differences between the two methods. There was still no strong evidence for onshore enhancement of abundance at this time. Rather, both methods showed a local maximum centered on stations S4–S7, in a strongly stratified region with shallow mixed layers $<25\,m$ (Fig. 2) and low nitrate. The hot spot seen in the microscope counts,

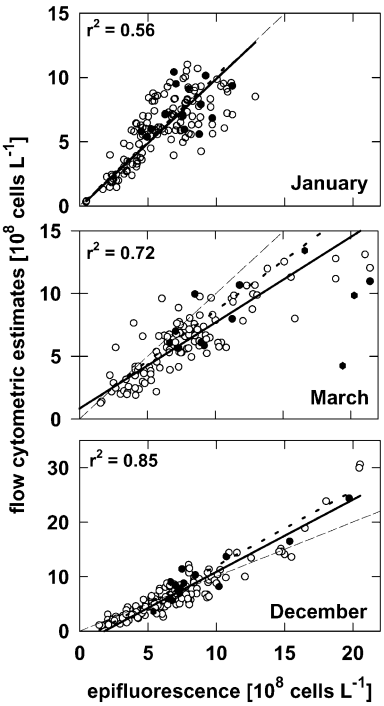

Fig. 3. Relationships between epifluorescent microscopic and flow cytometric determinations of heterotrophic bacterial abundance. All data points represent samples from the same Niskin bottles. Open circles, all data in upper 200 m (limit of sampling for cytometry). Solid symbols: surface data used in contour plots. There were no cytometric samples taken on the July cruise, and no microscopic samples on the August cruise. The Model II regressions (heavy solid lines) for the data are: January, $Y = 0.99X - 0.11 \times 10^8$, $r^2 = 0.564$, $n = 144$; March, $Y = 0.68X + 0.84 \times 10^8$, $r^2 = 0.72$, $n = 118$; December, $Y = 1.33X - 2.38 \times 10^8$, $r^2 = 0.85$, $n = 161$. The correlation coefficients for the surface data are: January, 0.20; March, 0.45, December, 0.89. Heavy dashed lines in March and December plots are Model II regressions for microscopic counts minus cytofluorometric prochlorophyte counts (see text). Light dashed lines are 1 : 1.

and mirrored in the distribution of leucine incorporation (Fig. 6) also had the highest observed levels of prochlorophyte abundance detected during the entire year. The flow cytometric observations suggested higher bacterial abundance extending from SW to NE, crossing from shallow to deeper mixed layers. The SW Monsoon was sampled during its mid- (July) and late (Aug. – Sept.) phases. Unfortunately, only one method for bacterial abundance could be employed on each of these two cruises. Bacterial abundance was high during the SW Monsoon, with a large region $> 15 \times 10^8$ cells l^{-1} in August (Fig. 4). In both July and August, peak abundances $> 10 \times 10^8$ cells l^{-1} covered the regions with high nitrate (cf. Fig. 2), but spread well beyond the nitrate-enriched area. There was little apparent spatial coincidence with the core of the low temperature (upwelling) fields or with mixed layer depth. The only consistent onshore enhancement of bacterial abundance was observed by both analyses in December, during the early NE Monsoon (Fig. 4, right-hand panels), and most of the offshore region again had lower abundance $< 10 \times 10^8$ cells l^{-1}, as in the previous January.

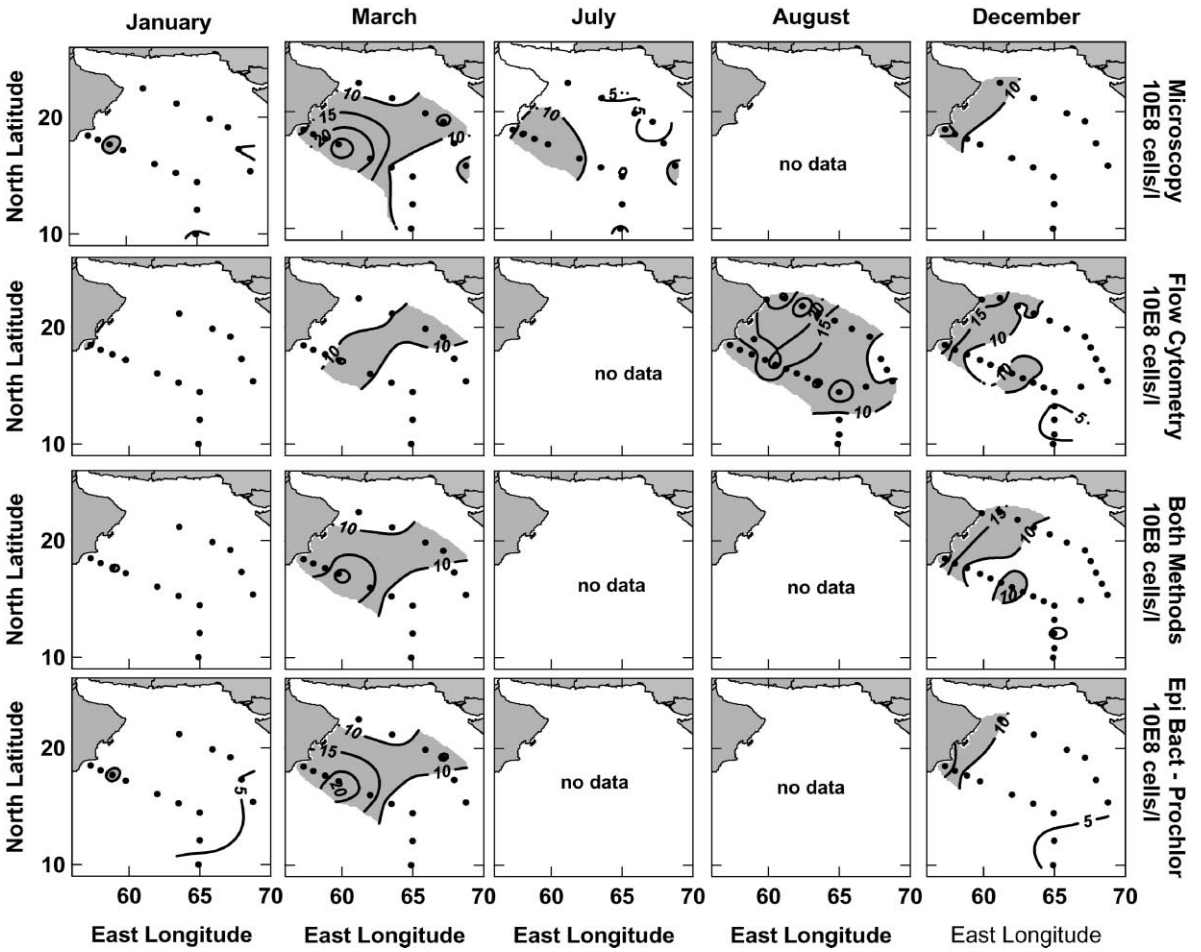

Fig. 4. Bacterial abundance distributions in the northern Arabian Sea surface, January–December, 1995, comparing determinations made by epifluorescence microscopy (top row) and flow cytometry (second row). The third row shows averaged contours using surface determinations by both methods. Only samples from stations where both analyses were performed were contoured in the combined December plot. The bottom row shows contours for microscopic counts minus cytofluorometric prochlorophyte counts. The contour interval is 5×10^8 cells/l. Shaded regions have abundance greater than 10^9 cells/l.

3.4. Cellular biovolume

Mean cell volumes were determined for all water column samples on the March and July cruises only. Cells were small, even for marine bacterioplankton, averaging $0.033\,\mu m^3$ cell^{-1} (SD, 0.009, $n = 654$, mean equivalent spherical diameter, 0.4 μm) for the two cruises. In contrast, cells in the Equatorial Pacific averaged 0.04–0.05 μm^3 cell^{-1} in the upper 50 m (Ducklow et al., 1995). In March, there was a distinct offshore maximum in cell volume with the largest cells > 0.030–0.035

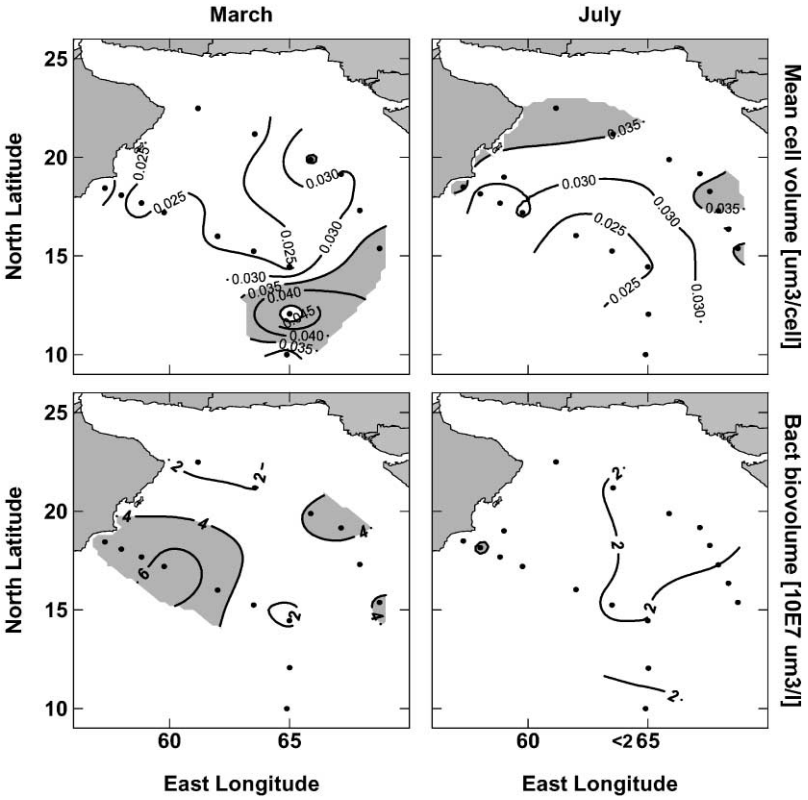

Fig. 5. Distribution of bacterial cell volume in the surface of the northern Arabian Sea surface. Measurements were only made on the March and July, 1995 cruises from image analyzed epifluorescence microscopy. Top panel, mean cell volume, contour interval $0.005\,\mu m^3$ per cell, shaded areas greater than $0.035\,\mu m^3$. Bottom panel, total bacterial biovolume (abundance times mean cell volume), contour interval, $10^7\,\mu m^3/l$, shaded areas greater than $4\times10^7\,\mu m^3/l$.

at the outer extent of the two transects (Fig. 5). In July cell volumes were more uniform with slightly larger cells in the north, generally in a region with mixed layers $< 50\,m$ (Fig. 2). Total bacterial biovolumes (abundance times mean cell volume) ranged from $1\text{–}8\times10^7\,\mu m^3 1^{-1}$ in March, reflecting the abundance distribution, but were uniformly low in July, when the gradients in volume opposed the abundance gradient (Fig. 5). Our cell volume estimates are considerably less than the $0.11\,\mu m^3$ value cited by Wiebinga et al. (1997), but the same as the $0.02\text{–}0.04\,\mu m^3$ found in our study area a year earlier by Pomroy and Joint (1998).

3.5. Bacterial production and growth rates

^{3}H-thymidine and ^{3}H-leucine incorporation rates were determined to estimate bacterial production throughout the water column at the rate process stations (large open and closed circles in Fig. 1) in January, March, July (south transect only) and December. Rates in the surface reported

Table 1
Rates of ^{3}H-thymidine and ^{3}H-leucine incorporation in the surface layer of the Arabian Sea. Each entry gives the mean (SD) and range in pmol $l^{-1}\,h^{-1}$

Month	^{3}H-Thymidine	^{3}H-Leucine	Ratio (Leu : TdR)
January ($n = 15$)	4.1 (2.3)	54 (45)	13.4 (6.2)
	1.4–8.7	19–202	5–28
March ($n = 14$)	5.1 (6.0)	46 (23)	12.4 (7.6)
	2–26	18–106	2–26
July ($n = 10$)	6.2 (3.4)	91 (46)	15.3 (5.9)
	4–16	6–169	2–23
December ($n = 15$)	1.8 (3.0)	45 (25)	59 (35)
	0.2–11	15–118	6–142

here varied greatly, with standard deviations of the same order as the means for all cruises (Table 1). Rates were not determined along the northern transect in July, but southern transect results suggest a maximum in leucine incorporation during the SW Monsoon (Table 1). Otherwise, rates were generally uniform during the year (Fig. 6). Leucine incorporation showed inshore maxima in January and December during the NE Monsoon. Thymidine incorporation was maximal in the northerly part of the study area in March, mirroring the distributions of temperature, nitrate and chlorophyll *a* (cf. Figs. 2 and 6). The cell-specific leucine incorporation rates, an index of biomass turnover rates, were similar in space and time to the incorporation rates, because of the greater dynamic range of the rates, compared to abundance measurements (Fig. 6). Leucine : thymidine incorporation rates, a rough indicator of cellular resource allocation (Shiah and Ducklow, 1997), were similar in January–July but differed conspicuously in December when thymidine incorporation was low (Table 1). The observed ranges of incorporation rates and ratios were similar to those reported by Wiebinga et al. (1997) and Pomroy and Joint (1998).

3.6. Subsurface maxima

In order to gain further insight into the geographic distributions of bacterial properties in the Arabian Sea, we examined the distribution and vertical location in the water column of subsurface bacterial abundance maxima (Figs. 4 and 7). Maxima were identified simply by locating the greatest abundance in the upper 200 m in each vertical profile determined by epifluorescence microscopy. The distribution of subsurface maxima closely mirrored the surface distributions, but of course with higher abundances at each station location (Fig. 7). The depth of the subsurface maximum layer was uniformly shoaler onshore in January, with inshore maxima at or near the surface (< 10 m) (Fig. 7, left column). The maxima were deeper in March during the Spring Intermonsoon when the region was more strongly stratified, and shallower during the SW Monsoon in July. Maxima were also shallow in December. In general, bacterial maxima were shallower, and had slightly lower amplitudes (ratio of mean maximum values to mean surface

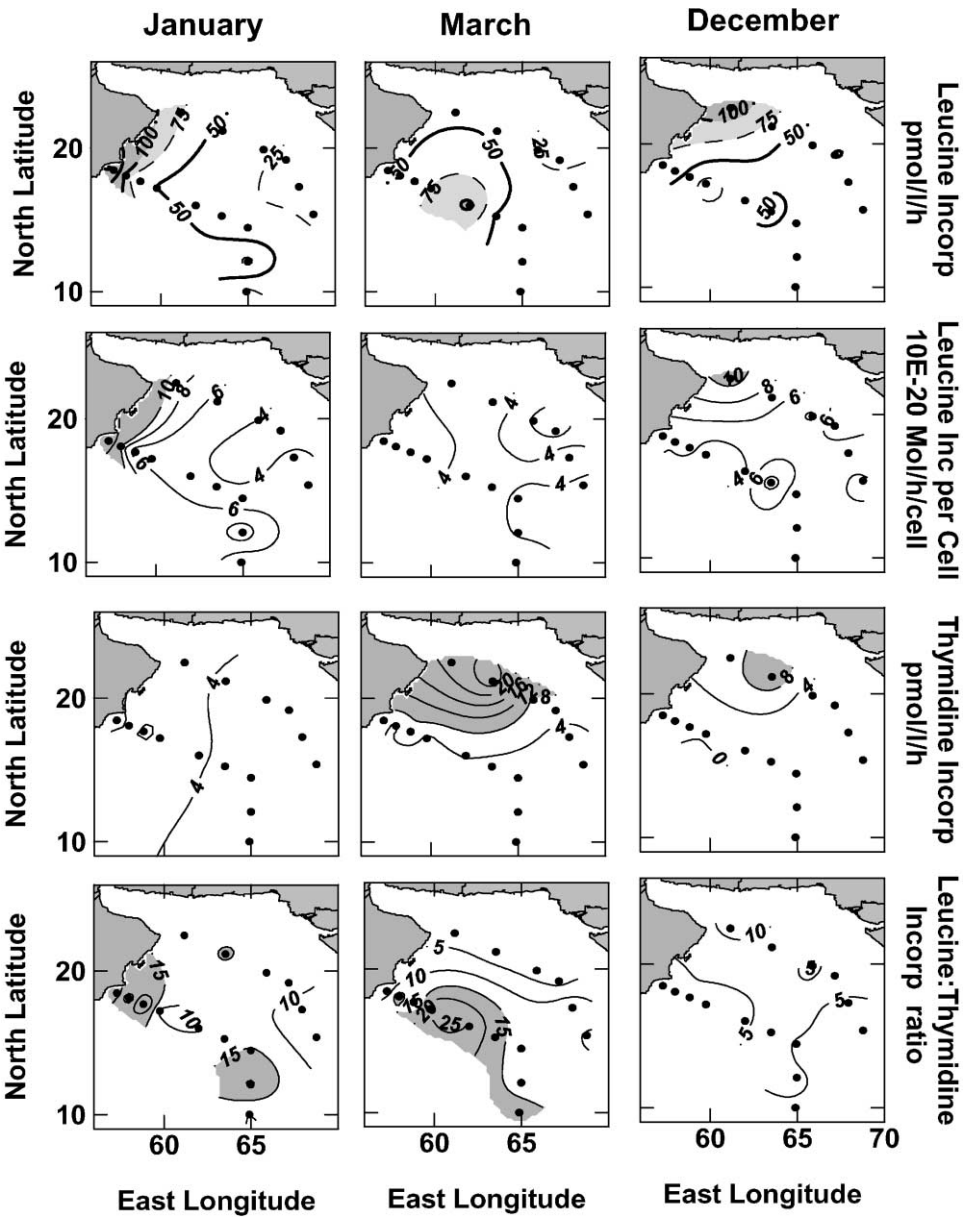

Fig. 6. Distribution of ^{3}H-leucine incorporation rates (top panel, contour interval, 25 pM h^{-1}, gray areas > 75); leucine incorporation per cell (second row, interval, 2×10^{-8} pM h^{-1} cell^{-1}, gray areas > 10); ^{3}H-thymidine incorporation rates (third row, contour intervals, 4 pM h^{-1}, gray areas > 8); leucine : thymidine incorporation ratio (bottom row, contour intervals, 5, gray areas > 15).

values) than subsurface chlorophyll *a* maxima (Table 2). Bacterial subsurface maxima were not pronounced (amplitudes < 1.3), but except for March, neither were the subsurface chlorophyll *a* maxima (Gundersen et al., 1998). Thus these maps reflect the general concentration of bacterial

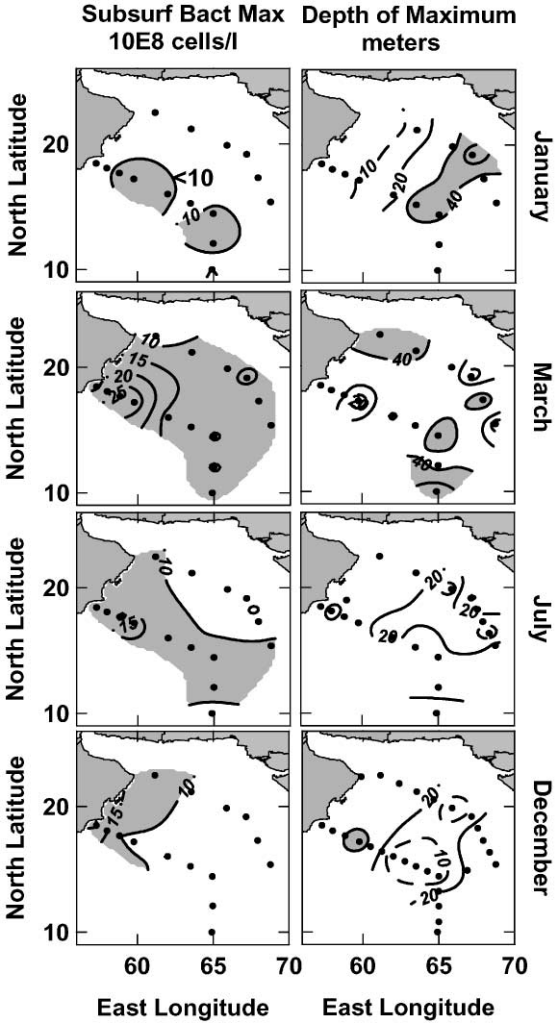

Fig. 7. Distribution of subsurface bacterial maxima in the Arabian Sea from epifluorescence microscopy. Left column, abundance at subsurface maximum (contour interval 5×10^8 cells l^{-1}, gray areas > 10 as in Fig. 4). Right column, depth of subsurface maxima, contour interval, 20 m, gray areas > 40 m.

biomass and activity in the surface mixed layer, and show more dramatically the enhancement of bacterial stocks in March, which stay relatively constant until the SW Monsoon period (Fig. 7).

4. Discussion

We were attracted to the Arabian Sea because we wanted to test general hypotheses about the regulation of heterotrophic carbon utilization in the open sea (Smith et al., 1991). In particular, we

Table 2
Subsurface bacterial and chlorophyll *a* maxima in the Arabian Sea, showing means of surface and subsurface properties at all stations sampled. The ratio of the value at the subsurface maximum to the surface value gives a measure of the amplitude of the subsurface maximum, if any existed. A value of 1 indicated maximum value at the surface. Bacterial abundance data from epifluorescence microscopy except August (FCM)

Month	Surface properties		Subsurface properties					
Number of stations	Bact	Chl[a]	Bact max	Bact Depth	Bact Max/Surf	Chl max	Chl Depth	Chl Max/Surf
	10^8 cells/l	μg/l	10^8 cells/l	m	ratio	μg/l	m	ratio
January ($n = 15$)	7.6	0.51	8.7	23.9	1.15	0.59	21.3	1.27
March ($n = 15$)	13.2	0.19	16.0	29.9	1.28	0.54	46.5	3.32
July ($n = 15$)	8.3	0.65	10.5	26.5	1.29	0.77	31.2	1.24
August ($n = 26$)	13.5	0.53	14.5	25.9	1.07	0.70	36.7	1.32
December ($n = 15$)	8.9	0.35	10.0	22.8	1.14	0.47	39.8	1.44

[a]HPLC Chl data obtained from the US JGOFS Database at http://usjgofs.whoi.edu/. Data originated by R. Bidigare and R. Goericke.

suggested that the anticipated strong response of the primary production system to coastal upwelling during the SW Monsoon would be a major influence on bacterial dynamics in the region (Azam et al., 1994), lasting perhaps through the following Fall Intermonsoon. Until recently there were few data sets to test this hypothesis. Chepurnova (1984) reported abundances from phase contrast microscopy of ca. 10^8–10^9 cells l^{-1} and derived biomass values of 20–70 μg C l^{-1} for cyclonic eddies in the central Arabian Sea, 10–15°N, 60–70°E,. The first modern investigation of bacterioplankton dynamics in the Indian Ocean was by Sorokin (1985), but it did not address the northwestern region most strongly influenced by monsoon wind forcing. Karrasch and Hoppe (1991) observed ca. 2×10^8 cells l^{-1} and production rates of 0.5–6 μg C l^{-1} d^{-1} (derived from TdR incorporation rates 0.2–2 pM hr^{-1}) near 18°N, 65°E during the late Spring Intermonsoon (April and May), 1987. These rates suggest the region was more oligotrophic than during our March 1995 cruise. Later Ducklow (1993) investigated bacterial ecology on a single cruise during the early Fall Intermonsoon in September–October, 1986, finding generally high levels of bacterial biomass and production for the open sea. Now, after four major JGOFS expeditions to the region we are in a better position to look critically at the seasonal patterns of bacterial dynamics, and possible mechanisms regulating them. We focus on the surface layer, where the bacterial populations are highest and most productive (Ducklow, 1993; Wiebinga et al., 1997; Pomroy and Joint, 1998; Campbell et al., 1998), to provide an overview of the geographical organization of seasonal bacterial dynamics.

4.1. Analysis of bacterial abundance

Campbell et al. (1998) provide the first regional scale view of bacterioplankton stocks using flow cytometry. Flow cytometry (FCM) offers several advantages over microscopy for oceanographic

investigation: ease of sampling, faster sample processing and simultaneous sensing of diverse cell populations (Campbell et al., 1994). On the other hand, epifluorescence microscopy provides ground truth for the FCM lasers, advantages of direct visual examination of samples, and coupled with image analysis, better resolution of cell volumes in the $< 0.1\,\mu m^3$ size range. We show here (Fig. 3) that the two methods detected comparable numbers of heterotrophic bacteria and provided essentially the same view of seasonal and spatial variation and pattern (but cf. Fig. 4, March panels). We noted cruise-specific and possibly approach-specific differences in March and December with slopes of 0.68 and 1.33, respectively, even though over all cruises, the two methods provided statistically indistinguishable results. Nonetheless, the between-cruise variability indicated that we cannot resolve subregional scale features in the bacterial distribution with certainty. For example, Fig. 4 shows several local bacterial maxima seen by one method but not the other. When the two methods differ greatly, as for example at Station S7 in December, the composite view will be weighted toward the higher value (Fig. 4, third row). In this paper we concentrate on the larger-scale, first-order features of seasonal changes and distributions that were detected consistently by the two approaches.

One major difference between the two approaches is in detecting prochlorophyte cells. These small autotrophs have the same size and cell morphology as heterotrophic bacteria, so acridine orange-stained cells will generally be counted as bacteria (Campbell et al., 1994). Their autofluorescence fades rapidly, preventing visual detection under the microscope, although they are captured in video microscopy. Inclusion of prochlorophyte counts as heterotrophic bacteria would provide an upward bias to the epifluorescence data, relative to the FCM analyses. To explore this bias, we subtracted the cytometric counts of prochlorophytes from the epifluorescence counts of bacteria. The hot spot near S4-7 in March, where FCM prochlorophyte counts were especially high is likely due to this effect in part (cf. March maps for uncorrected and corrected microscopic counts in Fig. 4). For the March data set, subtraction of prochlorophytes from the microscope counts raised the slope of the regression line slightly but significantly ($p < 0.05$; see short dashed line on plot, no significant change in r^2). For the other months, when the original slopes were > 1, correction of the microscope counts did not significantly alter the relationships. This analysis suggests that prochlorophyte interference was not a major cause of monthly or cruise-specific differences between microscope and FCM determinations, although the relationship was different in March. Contour plots of the corrected microscope data (Fig. 4, bottom row) show that although the magnitude of the estimates is reduced slightly, the areal distributions were not changed. Considering both methods together (Fig. 4, third row) gives the least biased, most representative version of the data.

4.2. Previous JGOFS research

Wiebinga et al. (1997) studied bacterial dynamics during the 1992–93 SW and NE Monsoons in the Gulf of Aden and the Somali Current. They found peak volumetric thymidine and leucine incorporation rates, and peak cell densities similar to those we observed, and concluded that bacterial production was supported by local primary production sources in both seasons. Their findings thus showed little need of our hypothesis (Ducklow, 1993; Azam et al., 1994) about the support of bacterial production by stored, semilabile DOC following monsoonal bloom periods. They found that bacterial properties were similar during the NE and SW Monsoons, with no bacterial bloom during the SW Monsoon. In drawing their conclusion about the relationship

between bacterial and primary production, Wiebinga et al. (1997) employed a rather high carbon per cell factor of 34 fg C, and also assumed a high growth efficiency of 50%. Conclusions about bacterial carbon fluxes remain critically dependent on largely unsupported assumptions about conversion factors and conversion efficiencies (Ducklow and Carlson, 1992). Employing a lower efficiency, but also a more central value for carbon per cell (20 fg C; Lee and Fuhrman, 1987) would generally preserve Wiebinga et al.'s (1997) overall conclusions that bacterial production was generally met by local sources of nutrition during the two monsoons.

Pomroy and Joint (1998) investigated bacterial carbon dynamics during the late SW Monsoon and following Fall Intermonsoon in 1994 in the same study area as US JGOFS, thus providing observations for a direct look at bacterial carbon demand relative to primary production during and following a monsoon-induced bloom. Like the observations presented here (Figs. 4 and 7) and those presented earlier by Ducklow (1993) and Wiebinga et al. (1997). Pomroy and Joint (1998) observed that bacterial abundance was generally high (ca. 0.8×10^9 cells l^{-1}) in the region north of 10°N during both seasons, consistent with our SW and NE Monsoon observations. Like Wiebinga et al. (1997), Pomroy and Joint (1998) did not observe a large pulse of bacterial production during the SW Monsoon. They presented several scenarios employing various combinations of conversion factors, and found that bacterial production was 10–30% of local primary production in both seasons. Pomroy and Joint (1998) observed that bacterial production and stocks did not change following the SW Monsoon. Both Wiebinga et al. (1997) and Pomroy and Joint (1998) found that levels of bacterial productivity and stocks were sustained following the peak in primary production. Further, both studies indicated that bacterial production was relatively low (10–20% of ^{14}C-PP) during the SW Monsoon, thus potentially allowing carbon storage for consumption during subsequent periods of lower productivity. Pomroy and Joint (1998) did find that their carbon demand estimates were greater than measurements of DOC release from phytoplankton made at the same stations, but noted that other DOC sources could make up the shortfall.

4.3. Was there a bacterial bloom during the SW Monsoon?

Wiebinga et al. (1997) showed similar levels of BP : PP during the NE and SW Monsoons in the Somali Current region, and Pomroy and Joint (1998) showed no great differences between the SW Monsoon and following Fall Intermonsoon in the northern Arabian Sea. Our own data suggest that bacterial abundance was high in the surface layer during the SW Monsoon, but not higher than during the Spring Intermonsoon (March, Figs. 4 and 7, and cf. Campbell et al., 1998). In contrast, bacterial stocks (i.e., cells m^{-2}) in the euphotic zone were highest during March (Table 3) and more uniform the rest of the year. High rates of bacterial productivity were found in different seasons, depending on which precursor (leucine or thymidine) was used (Fig. 6). Due to problems with isotope shipments, we were not able to provide a full areal picture for July, but data from the full southern transect indicate higher rates of incorporation in the surface layer in July (Table 1). Bacterial production in the euphotic zone derived from leucine incorporation rates, and also the ratio of BP/PP was highest in March *and* July (Table 3). Thus, in our data set, bacterial production showed just a small (< 2-fold) increase during the SW Monsoon, and stocks did not change, consistent with the observations by Wiebinga et al. (1997) and Pomroy and Joint (1998). Our observations do not preclude a further response following the SW Monsoon, as suggested by Ducklow (1993) but none of the data sets cited here were taken from the proper season to address

Table 3
Mean euphotic zone bacterial biomass (epifluorescence microscopy) and production[a] ($mMol\,C\,m^{-2}\,d^{-1}$) in the Arabian Sea, January–December, 1995

Cruise	cells/m^2	BP/m^2	EZ[b]	BP/PP	PP[c]
Jan ($n = 6$)	3.75×10^{13}	15.6	90	0.18	88.7
Mar ($n = 8$)	6.17×10^{13}	21.8	95	0.26	83.8
Jul ($n = 9$)	4.11×10^{13}	29.4	59	0.24	121.4
Dec ($n = 6$)	3.77×10^{13}	12.5	60	0.15	83.0

[a]Bacterial production derived from ^{3}H-leucine incorporation using $3\,kg\,C\,mol\,Leu^{-1}$ (Simon and Azam, 1989).
[b]Euphotic zone depth (meters).
[c]Mean of primary production at stations where BP was also measured.

the issue definitively. The data in our study suggest no bacterial bloom occurred during the SW Monsoon.

4.4. Did stored DOC support high bacterial production following the NE Monsoon?

Bacterial abundance rose sharply in March, following the NE Monsoon (Fig. 4), then declined slightly in the SW Monsoon (Table 3). BP increased by ca. 50% from January to March, and then by 30% until July (Table 3). The leucine : thymidine incorporation ratio was generally uniform at 10–15 from January through July (Fig. 6, July data for S transect not shown), suggesting roughly balanced growth throughout the first half of the year (Chin-Leo and Kirchman, 1990). These observations suggest that bacterial growth increased during the Spring Intermonsoon, while primary production stayed constant (Table 4).

Interestingly, US JGOFS observed relatively high levels of PP during *all* seasons, with just a small increase (40%) during the SW Monsoon (Table 4; Marra et al., 1998 and see cover image of Smith (1999). This is not entirely a novel finding. For example, Banse and English's (1993) reanalysis of CZCS fields showed that surface pigment was as high during the Spring Intermonsoon in March and April as in the preceding NE Monsoon or even higher in some parts of our study area (their regions 3 and 4 near our stations N4-7 and S7-11). There was a weak tendency for PP to be higher near the coast, but offshore transport of upwelled nutrients seemed to homogenize the PP field across the region (Banse, 1987). In our study, DOC (Table 4) was uniformly high (ca. $80\,\mu M$) in the surface layer throughout the study area between January and July, with just a slight decline in the latter half of the year. These values are somewhat higher than observed in the Sargasso and Ross Seas (Carlson et al., 1994; 1998), and the constancy of relatively high concentrations is remarkable. There was little seasonality in PP and DOC, as well as bacteria, in 1995. Overall, these observations suggest that high bacterial stocks and production in the (oligotrophic) Spring Intermonsoon were not enhanced by utilization of DOC stored from the previous monsoon. Rather, a longer term growth process commencing during the NE Monsoon was sustained during the Spring Intermonsoon as a result of continued high primary production. Slightly higher PP in July and August was not sufficient to trigger a notable bacterial bloom at that time.

Table 4
Mean primary productivity and euphotic zone chlorophyll a at main process stations, and surface DOC concentrations in the Arabian Sea, 1995

Month	Primary productivity[a] $m\,Mol\,C\,m^{-2}\,d^{-1}$		Euphotic zone Chl $mg\,m^{-2}$		Surface DOC $\mu Mol\,l^{-1}$	
	mean	SD	mean	SD	mean	SD
January	88.7	20.2	26	4	81	10
March	85.7	15.4	25	6	82	3
July	121.9	29.7	25	7	82	7
August	83.0	35.2	32	9	74	3
December	83.0	16.2	24	5	78	5

[a]Data in this Table were obtained from the US JGOFS Database at http://usjgofs.whoi.edu/. PP and Chl data originated by R. Barber and J. Marra. DOC data from D. Hansell and E. Peltzer.

5. Conclusion

A synthesis of these observations, including those made later (December) than previous studies, indicates an attenuated seasonal pattern qualitatively similar to that seen in subtropical, temperate and even polar regimes (Ducklow and Carlson, 1992): a winter minimum followed by a spring-summer increase of bacteria (Table 3). There is no evidence in our study, nor in previous investigations, of a strong (>2-fold) response of the bacterioplankton to the NE and SW Monsoons. We do find evidence for increases of bacterial stocks and production during the period following the NE Monsoon. Otherwise, bacterial stocks and production are high and roughly uniform in space and time, supported by year-round high levels of primary production and excess DOC (i.e., enhanced surface layer concentrations of labile and/or semilabile DOC above the deepwater values; Carlson and Ducklow, 1995). Intense grazing on picoplankton (Brown et al., 1999) combined with high DOM supply could poise bacterial abundance at uniformly high levels throughout the year, while maintaining the small cell sizes (ca. $0.033\,\mu m^3\,cell^{-1}$) we observed. High stocks of bacteria and high BP during the Spring Intermonsoon could be sustained on local PP which is higher than we originally anticipated for this period.

Acknowledgements

This research was supported by NSF OCE grants 9312695 to Azam, 9311246 to Landry and Campbell, 9612509 to Campbell and 9500601 to Ducklow. We are very grateful to German JGOFS colleagues Hans-Georg Hoppe and Soren Ullrich, Institut für Meereskunde, Kiel, for the very kind loan of ^{3}H-thymidine and ^{3}H-leucine transferred to us from R/V *Meteor* at sea near 10°N, 65°E on July 28. Their kindness, and the permission of research vessel officers to transfer radioisotopes via

Zodiac during the SW Monsoon allowed us to obtain valuable data on bacterial activity during this important season near the core of the upwelling system. Gary Schultz and Matt Church (VIMS) assisted with bacterial sampling in March and July. Flynn Cunningham assisted with epifluorescence microscopy performed at VIMS. Susan Brown, John Constantinou, Hector Nolla, and Hongbin Liu assisted with field sampling and FCM analyses. Finally, we cannot adequately express our thanks to our friends and colleagues Captain Glenn Gomes and the officers and crew of R.V. *T. G. Thompson* for dedicated support during a long and arduous campaign for an entire year, far from home.

This paper is contribution no. 531 from the US JGOFS Program.

References

Azam, F., Steward, G.F., Smith, D.C., Ducklow, H.W., 1994. Significance of bacteria in the carbon fluxes of the Arabian Sea. Proceedings of the Indian Academy of Sciences. Earth and Planetary Sciences 103, 341–351.

Banse, K., 1987. Seasonality of phytoplankton chlorophyll *a* in the central and northern Arabian Sea. Deep-Sea Research I 34, 713–723.

Banse, K., English, D.C., 1993. Revision of satellite-based phytoplankton pigment data from the Arabian Sea during the Northeast Monsoon. Marine Research 2, 83–103.

Bjornsen, P.K., 1986. Automatic determination of bacterioplankton biomass by image analysis. Applied Environmental Microbiology 51, 1199–1204.

Brock, J., Sathyendranath, S., Platt, T., 1993. Modeling the seasonality of subsurface light and primary production in the Arabian Sea. Marine Ecology Progress Series 101, 209–221.

Brock, J., Sathyendranath, S., Platt, T., 1994. A model study of seasonal mixed-layer primary production in the Arabian Sea. Proceedings of the Indian Academy of Sciences. Earth and Planetary Sciences 103, 163–176.

Brown, S.L., Landry, M.R., Barber, R.T., Campbell, L., Garrison, D.L., Gowing, M.M., 1999. Picophytoplankton dynamics and production in the Arabian Sea during the 1995 Southwest Monsoon. Deep-Sea Research II 46, 1745–1768.

Burkill, P.H., 1999. ARABESQUE: An Overview. Deep-Sea Research II 46, 529–548.

Campbell, L., Landry, M.R., Constantinou, J., Nolla, H.A., Brown, S.L., Liu, H., Caron, D.A., 1998. Response of microbial community structure to environmental forcing in the Arabian Sea. Deep-Sea Research II 45, 2301–2326.

Campbell, L., Nolla, H.A., Vaulot, D., 1994. The importance of Prochlorococcus to community structure in the central North Pacific Ocean. Limnology and Oceanography 39, 954–961.

Carlson, C.A., Ducklow, H.W., 1994. Annual flux of dissolved organic carbon from the euphotic zone in the northwestern Sargasso Sea. Nature 371, 405–408.

Carlson, C.A., Ducklow, H.W., 1995. Dissolved organic carbon in the upper ocean of the central equatorial Pacific Ocean, 1992: daily and finescale vertical variations. Deep-Sea Research II 42, 639–656.

Carlson, C.A., Ducklow, H.W., Smith, W.O., Hansell, D.A., 1998. Carbon dynamics during spring blooms in the Ross Sea polynya and the Sargasso Sea: contrasts in dissolved and particulate organic carbon partitioning. Limnology and Oceanography 43, 375–386.

Chepurnova, E.A., 1984. Bacterioplankton distribution in the euphotic zone of the northwest Indian Ocean from a mesoscale survey. Oceanology 24, 507–512.

Chin-Leo, G., Kirchman, D.L., 1990. Unbalanced growth in natural assemblages of marine bacterioplankton. Marine Ecology Progress Series 63, 1–8.

Ducklow, H.W., 1993. Bacterioplankton distributions and production in the Northwestern Indian Ocean and Gulf of Oman, September, 1986. Deep-Sea Research 40, 753–771.

Ducklow, H.W., Carlson, C.A., 1992. Oceanic bacterial productivity. Advances in Microbial Ecology 12, 113–181.

Ducklow, H.W., Quinby, H.L., Carlson, C.A., 1995. Bacterioplankton dynamics in the equatorial Pacific during the 1992 El Nino. Deep-Sea Research II 42, 621–638.

Gardner, W.D., Gundersen, J.S., Richardson, M.J., Walsh, I.D., 1999. The role of diel changes in mixed-layer depth on carbon and chlorophyll distributions in the Arabian Sea. Deep-Sea Research II 46, 1833–1859.

Goericke, R., Repeta, D.J., 1993. Chlorophylls *a* and *b* and divinyl chlorophylls *a* and *b* in the open Subtropical North Atlantic Ocean. Marine Ecology Progress Series 101, 307–313.

Goosen, N., van Rijswijk, K.P., de Bie, M., Peene, J., Kromkamp, J., 1997. Bacterioplankton abundance and production and nanozooplankton abundance in Kenyan coastal waters (Western Indian Ocean). Deep-Sea Research II 44, 1235–1250.

Gundersen, J.S., Gardner, W.D., Richardson, M.J., Walsh, I.D., 1998. Effects of monsoons on the seasonal and spatial distributions of POC and chlorophyll in the Arabian Sea. Deep-Sea Research II 45, 2103–2132.

Hobbie, J.E., Daley, R.J., Jasper, S., 1977. Use of Nuclepore filters for counting bacteria by fluorescence microscopy. Applied Environmental Microbiology 33, 1225–1228.

Karrasch, B., Hoppe, H.G., 1991. Vertical distribution and activity of bacteria in the Central Arabian Sea. Kiel Meeresforsch. (Sonderh.) 8, 74–80.

Knap, A., Michaels, A., Close, A., Ducklow, H., Dickson, A., (Eds.), 1996. Protocols for the Joint Global Ocean Flux Study (JGOFS) Core Measurements. JGOFS Report No. 19, vi + 170 pp. Reprint of the IOC Manuals and Guides No. 29, UNESCO 1994.

Latasa, M., Bidigare, R.R., Ondrusek, M.E., 1996. HPLC analysis of algal pigments: a comparison exercise among laboratories and recommendations for improved analytical performance. Marine Chemistry 51, 315–324.

Lee, S., Fuhrman, J.A., 1987. Relationships between biovolume and biomass of naturally-derived marine bacterioplankton. Applied Environmental Microbiology 52, 1298–1303.

Marra, J., Dickey, T.D., Ho, C., Kinkade, C.S., Sigurdson, D.E., Weller, R.A., Barber, R.T., 1998. Variability in primary production as observed from moored sensors in the central Arabian Sea in 1995. Deep-Sea Research II 45, 2253–2268.

Monger, B.C., Landry, M.R., 1993. Flow cytometric analysis of marine bacteria with Hoechst 33342. Applied Environmental Microbiology 59, 905–911.

Morrison, J., Codispoti, L.A., Gaurin, S., Jones, B., Manghanani, V., Zheng, Z., 1998. Seasonal variations of hydrographic and nutrient fields during the US JGOFS Arabian Sea Process Study. Deep-Sea Research II 45, 2053–2102.

Olson, D.B., Hitchcock, G.L., Fine, R.A., Warren, B.A., 1993. Maintenance of the low-oxygen layer in the central Arabian Sea. Deep-Sea Research II 40, 673–685.

Pomroy, A., Joint, I., 1998. Bacterioplankton activity in the surface waters of the Arabian Sea during and after the 1994 SW Monsoon. Deep-Sea Research II 46, 767–794.

Shiah, F.-K., Ducklow, H.W., 1997. Biochemical adaptations of bacterioplankton to changing environmental conditions: responses of leucine and thymidine incorporation to temperature and chlorophyll variations. Aquatic Microbial Ecology 13, 151–159.

Simon, M., Azam, F., 1989. Protein content and protein synthesis rates of planktonic marine bacteria. Marine Ecology Progress Series 51, 201–213.

Smith, D.C., Azam, F., 1992. A simple, economical method for measuring bacterial protein synthesis rates in seawater using 3H-leucine. Marine Microbial Food Webs 6, 107–114.

Smith, S.L., 25 Others, 1991. Arabian Sea Process Study. US Joint Global Ocean Flux Study Planning Report Number 12. Woods Hole: US JGOFS Planning Office. xi + 168 pp.

Smith, S.L., (Ed.), 1999. The 1994–1996 Arabian Sea Expedition: Oceanic Response to Monsoonal Forcing, Part 2. Deep-Sea Research II 46, 1531–1964.

Sorokin, Y.I., Kopylev, A.I., Mamaeva, N.V., 1985. Abundance and dynamics of the microplankton in the central tropical Indian Ocean. Marine Ecology Progress Series 24, 27–41.

Van Weering, T.C.E., Helder, W., Schalk, P., 1997. The Netherlands Indian Ocean Expedition 1992–1993, first results and an introduction. Deep-Sea Research II 44, 1177–1193.

Wiebinga, C.J., Veldhuis, M.J.W., De Baar, H.J.W., 1997. Abundance and productivity of bacterioplankton in relation to seasonal upwelling in the northwest Indian Ocean. Deep-Sea Research I 44, 451–476.

Yoder, J.A., McClain, C.R., Feldman, G.C., Esaias, W.E., 1993. Annual cycles of phytoplankton chlorophyll concentrations in the global ocean: a satellite view. Global Biogeochemical Cycles 7, 181–193.